Digital Compensation of Cross-Modulation Distortion in Multimode Transceivers

H.Habibi, Y. Wu, J. W. M. Bergmans
Eindhoven University of Technology
Department of Electrical Engineering
Signal Processing Systems
Email: H.Habibi@tue.nl

E. J. G. Janssen
Eindhoven University of Technology
Department of Electrical Engineering
Mixed-signal Microelectronics
Email: E.J.G.Janssen@tue.nl

***Abstract*—In a multimode transceiver, the transmitter for one communication standard induces a large interference on the receiver for another one. When this large interference passes through the inherently nonlinear receiver Front-End (FE), it introduces Cross-Modulation (CM) distortion. Increasing the FE linearity to lower the CM distortion leads to unacceptable power consumption for a handheld device. Considering the continuous increase of digital computation power governed by Moore's law an attractive alternative approach is to digitally compensate for the CM distortion. An existing CM compensation method is tailored to single-mode transceivers and requires an auxiliary FE. By using the locally available transmitted interference in the multimode transceiver, we propose a CM compensation method which requires no additional analog hardware. Hence the power consumption and complexity of the multimode transceiver will be reduced significantly.**

***Index Terms*—Multimode transceivers, Interference Mitigation, cross-modulation, digital compensation.**

I. Introduction

The number of communication standards supported by handheld devices has been increasing rapidly in the last years. To implement these standards, a combinations of several transceivers is required which is called a multimode transceiver [1]. In a multimode transceiver, the transmitter for one standard may be active at the same time with the receiver for another one. A sample scenario for a WLAN receiver (RX) and a WiMAX transmitter (TX) is shown in Fig. 1. The WiMAX transmitted signal $i_t(t)$ can be as high as 23 dBm while the received WLAN signal (desired signal $m_r(t)$) can be as low as -83 dBm [2]. The coupling loss between transceivers in a multimode transceiver is typically between 10 to 30 dB [3]. Hence the WiMAX TX induces an interfering signal $i_r(t)$ on the WLAN RX which can be 96 dB larger than $m_r(t)$.

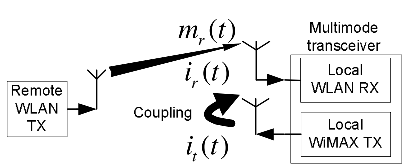

Fig. 1. A sample scenario in a multimode transceiver.

When the combination of $m_r(t)$ and $i_r(t)$ passes through the inherently nonlinear FE , nonlinear distortion products are generated, including harmonic, intermodulation and Cross-Modulation (CM) products. Unlike the other distortion products, the CM product always has the same center frequency as $m_r(t)$ and its power can be large enough to distort $m_r(t)$ significantly [4]. Therefore in this paper we focus on compensation of the CM distortion.

To reduce the power of nonlinear distortion products we can increase the FE linearity. Increasing the linearity for a certain input-referred noise, technology and circuit topology leads to additional power consumption [5]. Considering the limited energy supply in a handheld device increasing the power consumption will be impractical [6].

According to Moore's law the digital integrated circuits density is doubling every two years, resulting in cheaper computation power. On the other hand, the analog circuits chip area does not reduce so rapidly. Therefore, instead of increasing the FE linearity, a potentially attractive approach is to implement the FE with a linearity specification affordable in terms of power consumption for handheld devices, and digitally compensate for the CM distortion.

In [4] a method is reported to digitally compensate for the CM distortion in single-mode transceivers. In this method the received interfering signal, required for the CM compensation, is captured by an auxiliary FE and Analog to Digital Converter (ADC), leading to extra complexity and power consumption. However in the multimode transceiver the transmitted interfering signal is available locally and can be used to estimate the received interfering signal. This enables us to propose a CM compensation method with no auxiliary FE and ADC, at the expense of slightly higher complexity in the digital domain. As a result the chip area and power consumption of the multimode receiver will be significantly reduced compared to [4]. Also instead of using pilot symbols of $m_r(t)$ to estimate the CM distortion as [4], the proposed method is based on the statistical independence of $m_r(t)$ and $i_r(t)$. Hence it can also be used in the absence of pilot symbols. The simulation results demonstrate that the proposed method can lower distortion to a negligible level at realistic interference levels.

II. System Model

The direct conversion receiver architecture is a popular choice for implementation in integrated circuits. Fig. 2 shows

978-1-4673-0990-5/12/$31.00 ©2012 IEEE

such a receiver tuned to the center frequency f_0 of $m_r(t)$ in Fig. 1. The received signal $x_r(t)$ is collected by an antenna and is passed through a bandpass filter (BPF) to limit the input frequency range. The BPF output $x_{\text{bp}}(t)$ is amplified by a Low Noise Amplifier (LNA). The amplified signal $y(t)$ is down-converted to zero frequency by an ideal quadrature mixer with local oscillator frequency of f_0. The complex output $y_d(t)$ of the mixer is filtered by a lowpass filter (LPF) to select a certain frequency channel. The LPF complex output $z(t)$ is sampled by an ADC with a sampling period of T_s seconds. The ADC output $z[p_s]$ is processed in a digital baseband processor to extract the transmitted information. The symbol p_s is used for the indices that belong to the clock domain T_s.

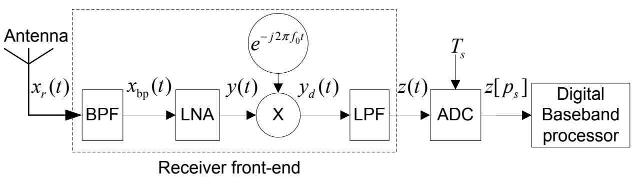

Fig. 2. Direct conversion receiver.

As shown in Fig. 1, the front-end input $x_r(t)$ is the combination of $m_r(t)$ and $i_r(t)$. The complex baseband interfering signal $i[p_i]$ is converted to a continuous signal $i(t)$ with a conversion period T_i , up-converted to a carrier frequency f_1, transmitted by the local TX antenna as $i_t(t)$ and, after a path loss and a phase shift is received by the local RX antenna as $i_r(t)$. Because of the small distance between the local TX and RX antennas any propagation delay is neglected.

The BPF effect on $m_r(t)$ can be taken as part of the communication channel. Here we assume that the BPF effect on $i_r(t)$ can be modeled as an attenuation and phase shift. By accepting this assumption the combined effect of the TX-RX path and the BPF on $i_t(t)$ can be modeled as multiplication by a priori unknown complex number α_i. Hence $x_{\text{bp}}(t)$ can be written as:

$$x_{\text{bp}}(t) = \text{Re}\left\{ \left(m(t) + \alpha_i i(t) e^{2\pi j (\Delta f) t} \right) e^{2\pi j f_0 t} \right\}, \qquad (1)$$

where $m(t)$ is the baseband equivalent of $m_r(t)$ and $\Delta f = f_1 - f_0$. Because degradation in the performance of the receiver for moderate and high signal to noise ratios is dominated by the interference [4], the input noise is neglected in (1). It is common to model the input-output relation of the LNA by a third-order polynomial as [4]:

$$y(t) = a_1 x_{\text{bp}}(t) + a_3 x_{\text{bp}}^3(t), \qquad (2)$$

where a_1 is the LNA small signal gain and the value of a_3 shows amount of the LNA nonlinearity. Without loss of generality, in the rest of this paper we will assume that $a_1 = 1$.

Using (2) and (1), $y_d(t)$ in Fig. 2 can be written as:

$$\begin{aligned} y_d(t) = {} & m(t) + \frac{3}{4} a_3 m(t) |m(t)|^2 \\ & + \frac{3}{2} a_3 |\alpha_i|^2 m(t) |i(t)|^2 \\ & + \text{Components centered at } \pm\Delta f,\ 2\Delta f \\ & + \text{High frequency components around } 2f_0,\ 2f_1\ . \end{aligned} \qquad (3)$$

In (3), the second term is the harmonic product and the third term is the CM product. In this paper we assume that:

1) The frequency separation Δf is large enough that the components in (3) centered at $\pm\Delta f$ and $2\Delta f$ do not have any spectral overlap with $m(t)$ and are filtered out by the LPF.
2) The FE is designed to process $m_r(t)$ with negligible nonlinear distortion in the absence of $i_r(t)$. Hence $\frac{3}{4} a_3 m(t) |m(t)|^2$ is negligible compared to $m(t)$.
3) To simplify the CM compensation, we choose the bandwidth B_{LPF} of the LPF large enough to pass the CM product without distortion.

Using the above practical assumptions, $z(t)$ can be approximated by:

$$z(t) \simeq m(t) \left(1 + d |i(t)|^2 \right), \qquad (4)$$

where d is defined as:

$$d = \frac{3a_3}{2} |\alpha_i|^2. \qquad (5)$$

According to (4) the CM distortion can be seen as an unwanted amplitude modulation of the desired signal. Most active circuits (e.g. LNA) have compressive behavior so that $a_1 a_3 < 0$. Hence d will be a negative number. According to (5) d depends on a_3, α_i. Variations in the value of a_3 and α_i originate from variations of circuit parameters (e.g. temperature) or changes happening in the handheld device environment (e.g. presence of the user hand can change the coupling in Fig. 1). Therefore d can be assumed constant for time spans in the order of 1 ms.

By sampling $z(t)$ with a rate high enough to prevent aliasing ($\frac{1}{T_s} > B_{\text{LPF}}$), the resulting discrete-time signal will be:

$$z[p_s] = z(t)|_{t = p_s T_s} \simeq m[p_s] \left(1 + d |i[p_s]|^2 \right), \qquad (6)$$

where

$$m[p_s] = m(t)|_{t = p_s T_s}, i[p_s] = i(t)|_{t = p_s T_s}. \qquad (7)$$

The approximate model of the CM distortion based on (6) and (7) is illustrated in Fig. 3. The output of the ADC for an exactly linear FE would be $m[p_s]$. Because of the CM distortion $m[p_s]$ is multiplied by $1 + d|i[p_s]|^2$, where $i[p_s]$ is generated by a Sampling Rate Conversion (SRC) of $i[p_i]$ from sampling period T_i to T_s.

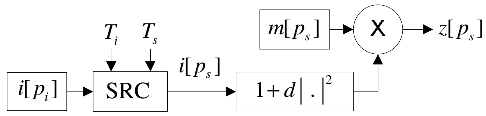

Fig. 3. Approximate model of the CM distortion based on (6).

III. Proposed compensation method

According to (6), by dividing $z[p_s]$ by $(1 + d|i[p_s]|^2)$ the CM distortion can be compensated. Hence the core part of our compensation method is to estimate $(1 + d|i[p_s]|^2)$. The proposed compensation scheme is illustrated in Fig. 4. The SRC re-samples $i[p_i]$ from the sampling period T_i to T_s. Then d is estimated by processing $z[p_s]$ and $i[p_s]$ together, as explained below. The estimated value of $\hat{d}$ is used to calculate $(1 + \hat{d}|i[p_s]|^2)$. The CM compensation is done by dividing $z[p_s]$ by $(1 + \hat{d}|i[p_s]|^2)$. The compensated signal $\hat{m}[p_s]$ will be processed as usual by the following stages of the receiver.

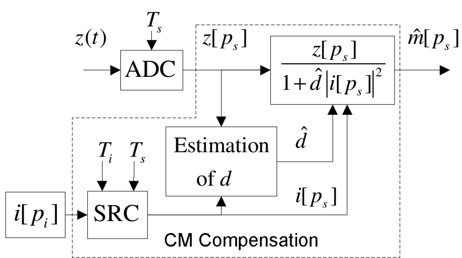

Fig. 4. Proposed compensation scheme.

In this section we replace $\simeq$ in (6) with $=$ to clarify where new approximations are made. Here we estimate d, where $i[p_s]$ and $z[p_s]$ are known and $m[p_s]$, $p_s = 1..N$ is unknown. Because $m[p_s]$ and $i[p_s]$ originate from two independent transmitters they can be assumed to be statistically independent. Taking the absolute value of both sides of (6) results in:

$$|z[p_s]| = |m[p_s]| \left(1 + d|i[p_s]|^2\right). \tag{8}$$

Here we assumed that $1 + d|i[p_s]|^2$ is positive. The factor $(1 + d|i[p_s]|^2)$ represents the effective gain that $m[p_s]$ experiences. For a normal amplifier, this gain decreases from the small-signal gain ($a_1 = 1$) in the absence of the interfering signal to zero when $|i[p_s]|$ becomes very large. Now define E_k, $E_{|m|}$ and I_k as:

$$\begin{aligned} &E_{|m|} = E\{|m[p_s]|\}, I_k = E\{|i[p_s]|^k\} \\ &E_k = E\{|z[p_s]i[p_s]|^k\}. \end{aligned} \tag{9}$$

Taking the expected value of both sides of (8) results in:

$$E_0 = E_{|m|}(1 + dI_2). \tag{10}$$

Multiplying both sides of (8) by $|i[p_s]|$ and taking the expected value results in:

$$E_1 = E_{|m|}(I_1 + dI_3). \tag{11}$$

Dividing (10) by (11) and solving for d results in:

$$d = \frac{E_0 I_1 - E_1}{I_2 E_1 - I_3 E_0}. \tag{12}$$

To calculate the expected values in (12) we need the exact probability distributions of $m[p_s]$ and $i[p_s]$, which are unknown. Instead the expected values can be approximated by their corresponding time averages as:

$$\hat{E}_k = \frac{1}{N}\sum_{p_s=1}^{N} |z[p_s]i[p_s]|^k, \hat{I}_k = \frac{1}{N}\sum_{p_s=1}^{N} |i[p_s]|^k, \tag{13}$$

where N is the number of samples used in the estimation. Using these approximated values d can be estimated as:

$$\hat{d} = \frac{\hat{E}_0 \hat{I}_1 - \hat{E}_1}{\hat{I}_2 \hat{E}_1 - \hat{I}_3 \hat{E}_0}. \tag{14}$$

Writing (10) and (11) in terms of time averages introduces error terms to both equations proportional to $\frac{1}{N}$ multiplied by the varaince of $|m[p_s]|$ [7]. Therefore the error in estimating d will be proportional to $\frac{1}{N}$ and becomes larger for modulations of $m[p_s]$ with more envelope variations.

IV. Simulation results

For simulation we consider the scenario of Fig. 1 with the following parameters:

- The WLAN received signal $m_r(t)$: $f_0 = 2462$ MHz, 20 MHz bandwidth and -60 dBm power.
- The WiMAX transmitted signal $i_t(t)$: $f_1 = 2501$ MHz, 10 MHz bandwidth and maximum power of 23 dBm.
- The coupling loss : -20 dB, The BPF Attenuation on $i_r(t)$:23 dB.
- The WLAN FE third-order Input Intercept Point(IIP3): -10 dBm, equivalent to $a_3 = -133$.

Using the above parameters, d is limited to $[-0.20, 0]$, where 0 and -0.20 correspond to zero and maximum interference levels, respectively. Simulations are performed for three types of modulation for $m[p_s]$: single carrier QPSK, 64QAM and 64 sub carrier OFDM with 64 QAM for each sub-carrier. Zero mean, unit variance Circularly-Symmetric Gaussian (CSG) random signals are used for $i[p_s]$, which approximates a baseband OFDM signal. The received signal $z[p_s]$ is generated via the simplified model in Fig. 3.

The Signal to Distortion Ratio for $z[p_s]$, SDR$\{z\}$, can be defined as the power ratio of $m[p_s]$ and CM product as:

$$\begin{aligned} \mathrm{SDR}\{z\} &\triangleq \frac{E\{|m[p_s]|^2\}}{E\{|dm[p_s]|i[p_s]|^2|^2\}} \\ &= \frac{1}{d^2 E\{|i[p_s]|^4\}}. \end{aligned} \tag{15}$$

When $i[p_s]$ is a zero mean unit variance CSG random signal then $E\{|i[p_s]|^4\} = 2$ [4] and (15) can be written as:

$$\mathrm{SDR}\{z\} = \frac{1}{d^2 E\{|i[p_s]|^4\}} = \frac{1}{2d^2}. \tag{16}$$

According to (16), SDR$\{z\}$ only depends on d. In this scenario SDR$\{z\} \geq 11$ dB, where the equality happens for $d = -0.2$.

The MSE$\{\hat{d}\}$ versus SDR$\{z\}$ is shown in Fig. 5 for $N = 10^3, 10^4$. Two trends are observed for SDR$\{z\} > 16$ dB and SDR$\{z\} < 16$ dB. For SDR$\{z\} > 16$ dB the main source of error originates from replacing expected values with times averages. The MSE$\{\hat{d}\}$ is slightly decreased by decreasing SDR$\{z\}$. Hence we have a smaller error in estimation of d for larger amounts of the CM distortion. The MSE$\{\hat{d}\}$ is proportional to $\frac{1}{N}$ (i.e. becomes 10 times samller by increasing N 10 times) and is larger for the modulations with more envelope variations. For SDR$\{z\} < 16$ dB the MSE$\{\hat{d}\}$ increases by decreasing the SDR$\{z\}$. This phenomenon originates from our assumption on the positivity of $1 + d|i[p_s]|^2$ in (8). Because here $i[p_s]$ has a Gaussian distribution this assumption does not always hold. Violaiting this assumtion generates an error term that becomes dominant for SDR$\{z\}$ <16 dB.

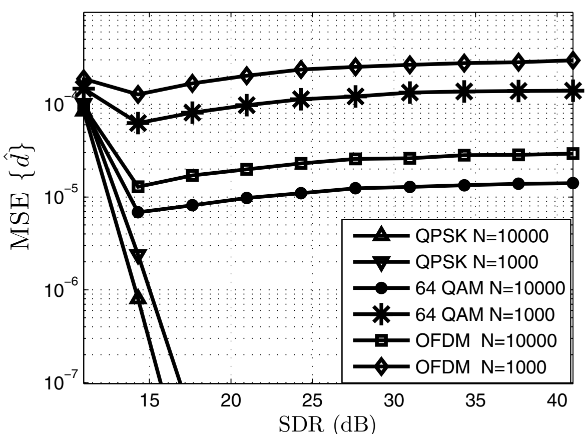

Fig. 5. MSE$\{\hat{d}\}$ versus SDR$\{z\}$ for $N = 10^3, 10^4$.

In Fig. 6 the uncoded Symbol Error Rate (SER) is shown versus SDR$\{z\}$. With compensation the SDR of 64 QAM modulation is improved by 15 dB, equivalent to 7.5 dB improvement in the effective IIP3 of the FE. Compared to 64 QAM, OFDM shows a smaller improvement in SDR after compensation, about 10 to 8 dB. QPSK modulation shows the smallest improvement. The reason is that the occasional errors of QPSK modulated signal happen when $1 + d|i[p_s]|^2$ is close to zero and an small error of $\hat{d}$ can change the sign of $1 + \hat{d}|i[p_s]|^2$, leading to incorrect compensation.

V. Conclusion

Based on the simplified models for the FE nonlinearity and transmit-receive path of the interfering signal, a discrete-time model for the received signal in multimode transceivers is presented. Based on this a CM compensation method is proposed. The simulation results show the effectiveness of the method to improve the receiver's SER in the presence of the interfering signal for different modulations of the desired signal. The proposed method can be used in current multimode transceivers to reduce the power consumption with minimum modification.

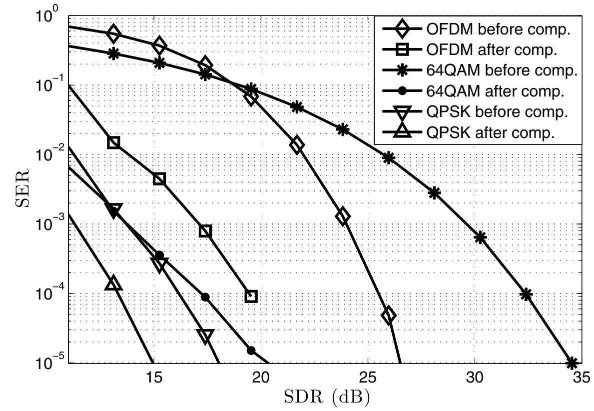

Fig. 6. SER versus SDR$\{z\}$ before and after compensation.

Acknowledgment

This work was funded by the Netherlands technology foundation (STW) within Digitally Enhanced And Controlled Front-Ends (DECAFE) project.

References

[1] D. Robertson and T. Montalvo, "Issues and trends in rf and mixed signal integration and partitioning," *Communications Magazine, IEEE*, vol. 46, no. 9, pp. 52 –56, sep. 2008.

[2] L. Maurer, "Adaptive digital front-end enhanced cmos-based rf transceivers a brief overview," nov. 2008, pp. 111 –114.

[3] J. Zhu, A. Waltho, X. Yang, and X. Guo, "Multi-radio coexistence: Challenges and opportunities," aug. 2007, pp. 358 –364.

[4] Q. Zou, M. Mikhemar, and A. Sayed, "Digital compensation of cross-modulation distortion in software-defined radios," *Selected Topics in Signal Processing, IEEE Journal of*, vol. 3, no. 3, pp. 348 –361, jun. 2009.

[5] W. Sheng, A. Emira, and E. Sanchez-Sinencio, "Cmos rf receiver system design: a systematic approach," *Circuits and Systems I: Regular Papers, IEEE Transactions on*, vol. 53, no. 5, pp. 1023 – 1034, may. 2006.

[6] A. Dejonghe, B. Bougard, S. Pollin, J. Craninckx, A. Bourdoux, L. Ven der Perre, and F. Catthoor, "Green reconfigurable radio systems," *Signal Processing Magazine, IEEE*, vol. 24, no. 3, pp. 90 –101, may. 2007.

[7] G. Box, G. M. Jenkins, and G. Reinsel, *Time Series Analysis: Forecasting & Control (3rd Edition)*, 3rd ed. Prentice Hall, 1994.